

Supporting Information

3D Ordered Macroporous Copper Nitride-Titanium Oxynitrides as Highly Efficient Electrocatalysts for Universal-pH Hydrogen Evolution Reaction

Yuchen Wu^{1,2}, Fanghua Ning³, Zhiwei Wang^{1,2}, Ali Saad², Xiuting Li^{*1} and Dingguo Xia^{*3}

¹ *Institute for Advanced Study, Shenzhen University, Shenzhen 518060, China.*

² *Key Laboratory of Optoelectronic Devices and Systems, College of Physics and Optoelectronic Engineering, Shenzhen University, Shenzhen 518060, China.*

³ *Beijing Key Laboratory of Theory and Technology for Advanced Batteries Materials, School of Materials Science and Engineering, Peking University, Beijing 100871, P. R. China.*

*Correspondence and requests for materials should be addressed to X.L. (email: xiuting.li@szu.edu.cn) or to D.X. (email: dgxia@pku.edu.cn).

Table of Contents

Fig. S1 Calibration curve of SCE vs RHE in 0.5M H ₂ SO ₄ , 1M PBS and 1M KOH electrolyte solution.	3
Fig. S2 (a)SEM, (b) TEM of Cu ₃ N(20)@3DOM-TiO _x N _y at low magnitude.....	4
Fig. S3 TEM scanning of Cu ₃ N(20)@3DOM-TiO _x N _y , a) Electron layered image, b) TEM image, EDS mapping of c) Ti, d) Cu, e) N, f) O, g) C, and i) atomic ratio.	5
Fig. S4 N ₂ ad/desorption isotherm of bulk-Cu ₃ N(20)@TiO _x N _y	6
Fig. S5 CV and specific capacitance curve of Cu ₃ N(20)@3DOM-TiO _x N _y under scan rates from 1 mV s ⁻¹ to 100 mV s ⁻¹	7
Fig. S6 (a) XPS survey, and (b) C1s scan of Cu ₃ N(20)@3DOM-TiO _x N _y	8
Fig. S7 Broken 3DOM porous structure of Cu ₃ N(40)@3DOM-TiO _x N _y	9
Fig. S8 Water splitting electrolyzer using Cu ₃ N(20)@3DOM-TiO _x N _y electrocatalyst cathode.....	10
Table S1 Ti and Cu ratio obtained from ICP-OES test.	11
Table S2 Surface area, pore distribution and pore volume comparison of Cu ₃ N(20)@3DOM-TiO _x N _y and bulk-Cu ₃ N(20)@TiO _x N _y	12
Table S3 Surface elemental weight ratio and atomic ratio of the C, N, O, Ti, Cu and Cl.	13
Table S4 HER performance comparison of several up to date related electrocatalysts.	14
References	15

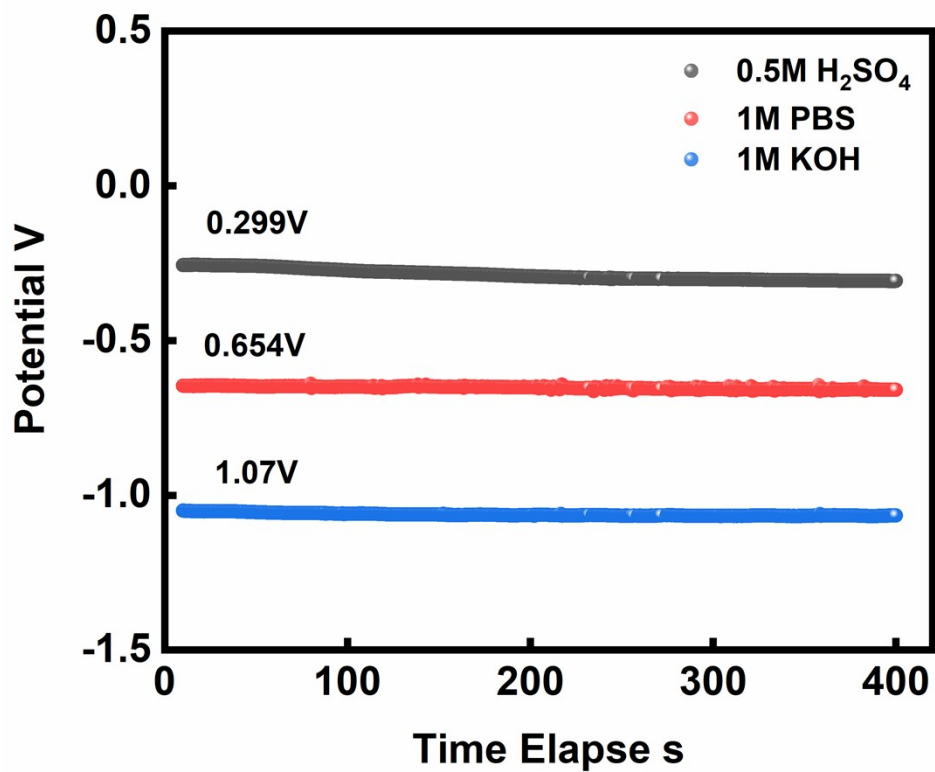


Fig. S1 Calibration curve of SCE vs RHE in 0.5M H₂SO₄, 1M PBS and 1M KOH electrolyte solution.

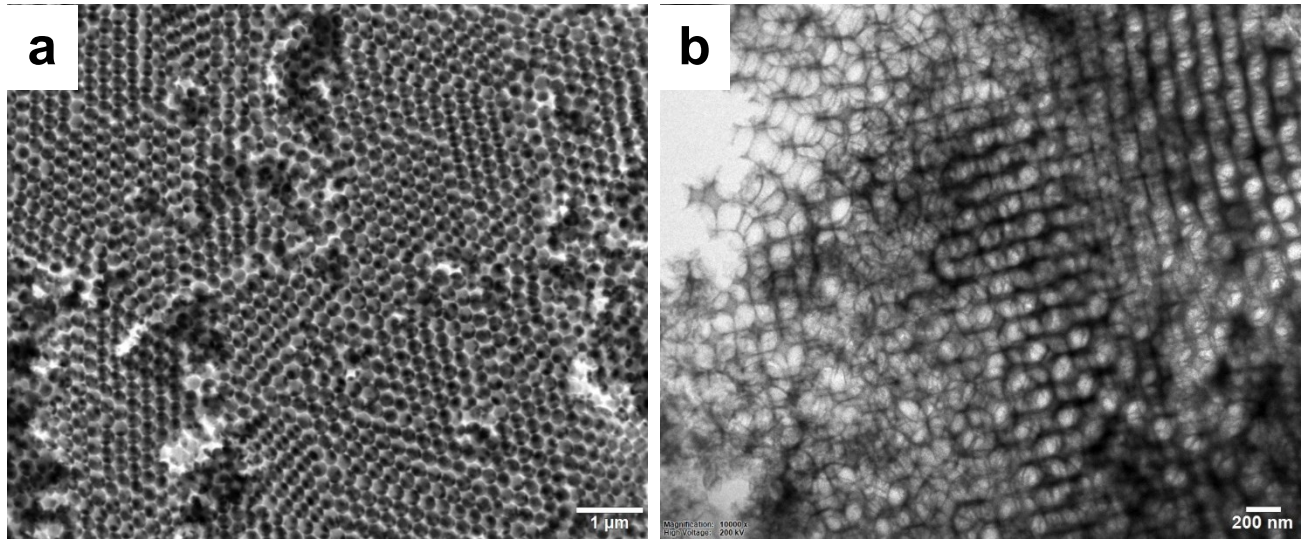


Fig. S2 (a)SEM, (b) TEM of $\text{Cu}_3\text{N}(20)\text{@}3\text{DOM-TiO}_x\text{N}_y$ at low magnification.

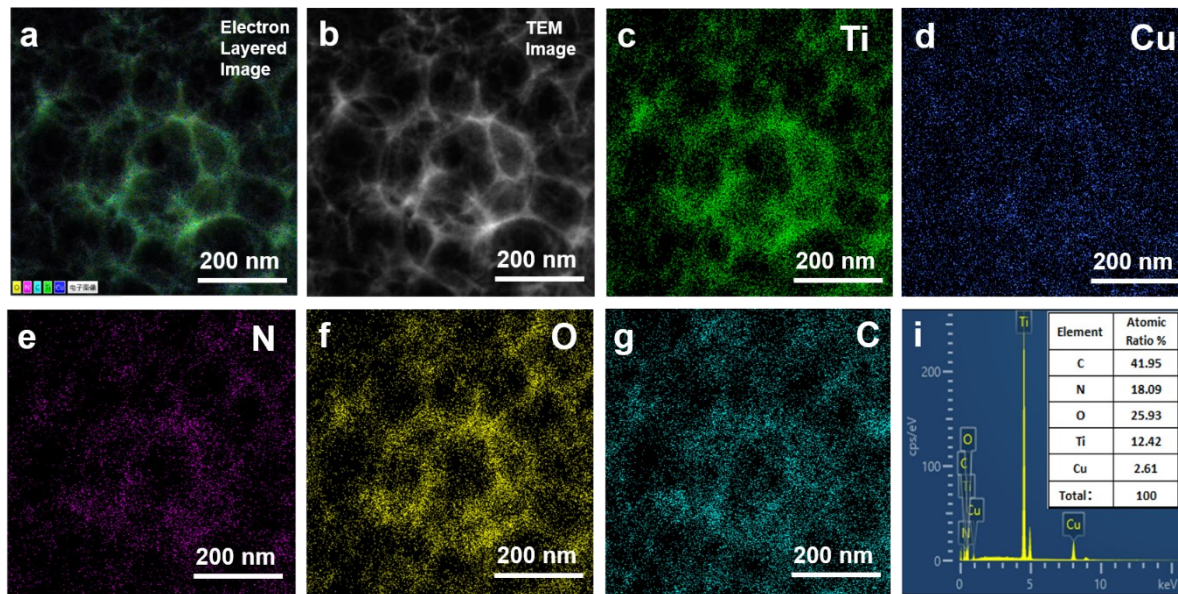


Fig. S3 TEM scanning of $\text{Cu}_3\text{N}(20)\text{@}3\text{DOM-TiO}_x\text{N}_y$, a) Electron layered image, b) TEM image, EDS mapping of c) Ti, d) Cu, e) N, f) O, g) C, and i) atomic ratio.

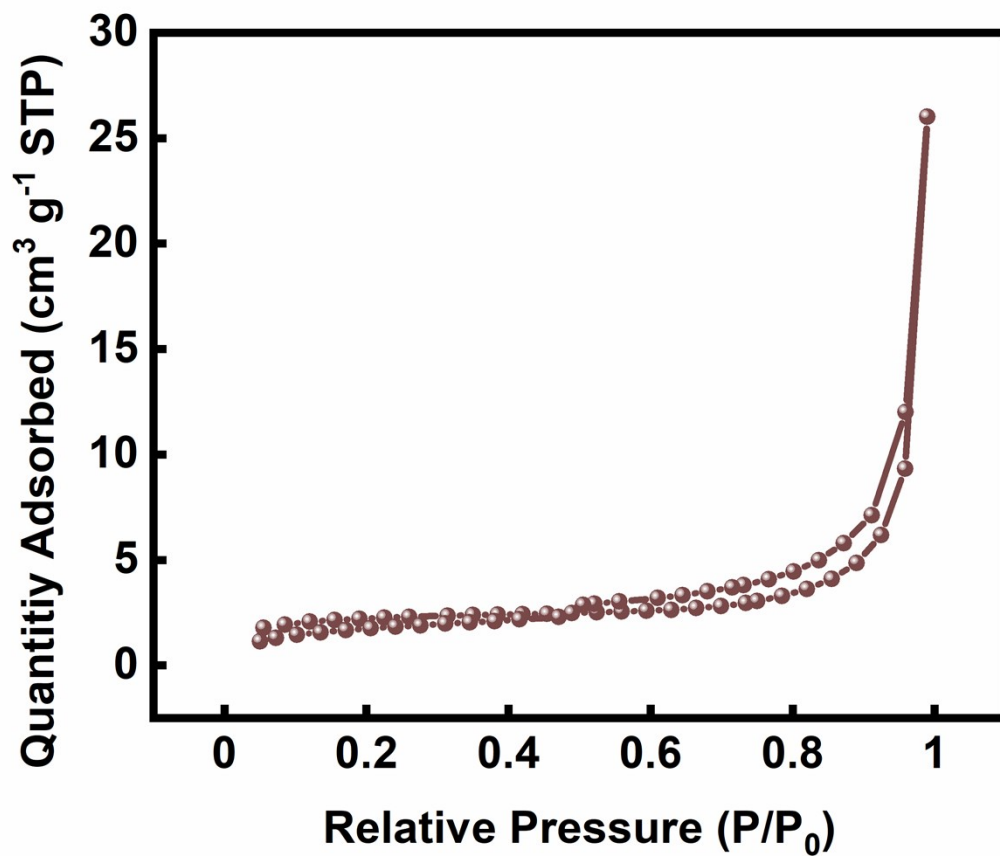


Fig. S4 N₂ ad/desorption isotherm of bulk-Cu₃N(20)@TiO_xN_y.

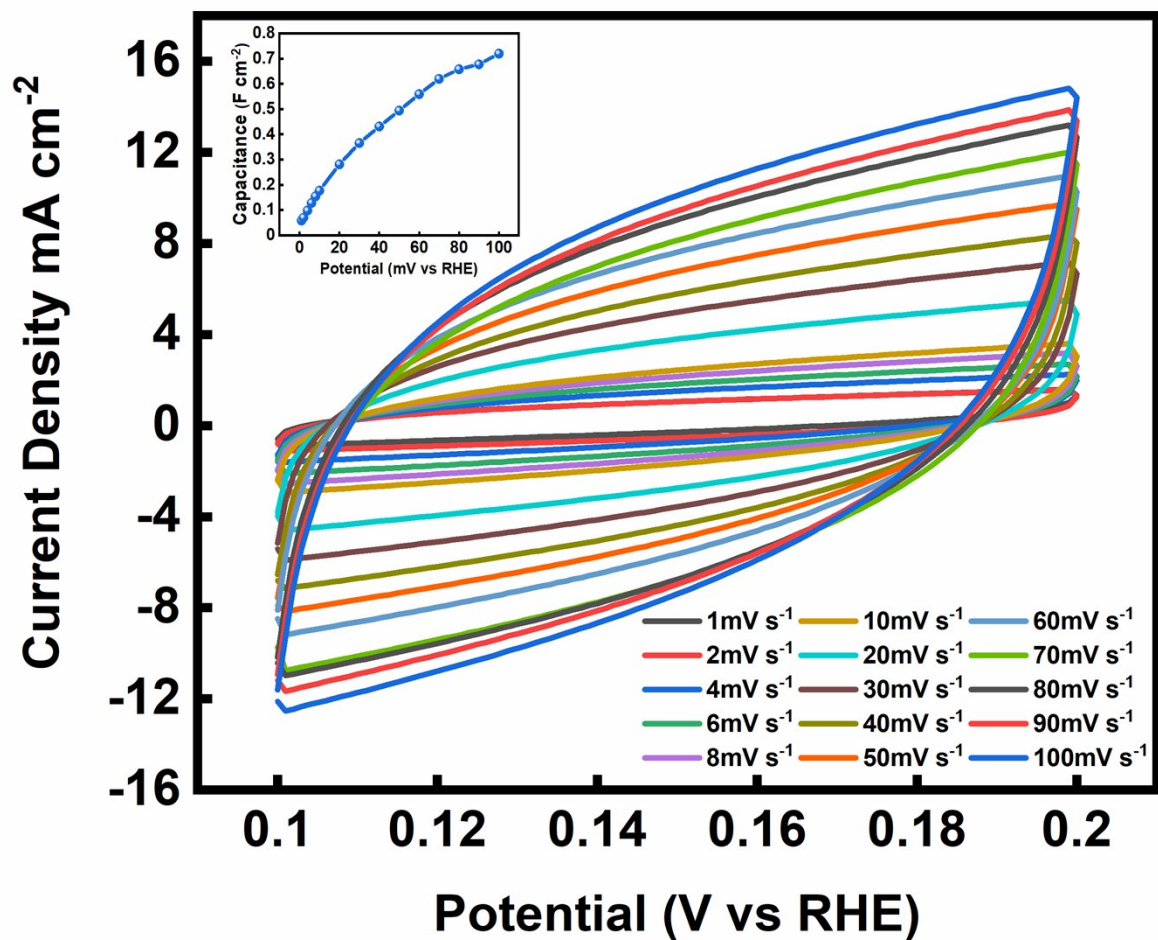


Fig. S5 CV and specific capacitance curve of Cu₃N(20)@3DOM-TiO_xN_y under scan rates from 1 mV s⁻¹ to 100 mV s⁻¹.

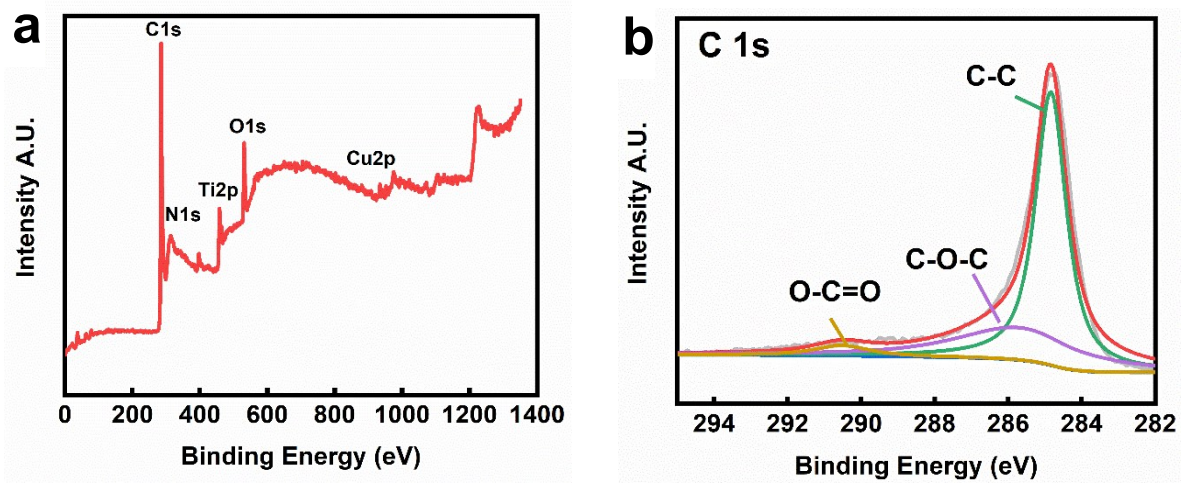


Fig. S6 (a) XPS survey, and (b) C1s scan of $\text{Cu}_3\text{N}(20)\text{@}3\text{DOM-TiO}_x\text{N}_y$.

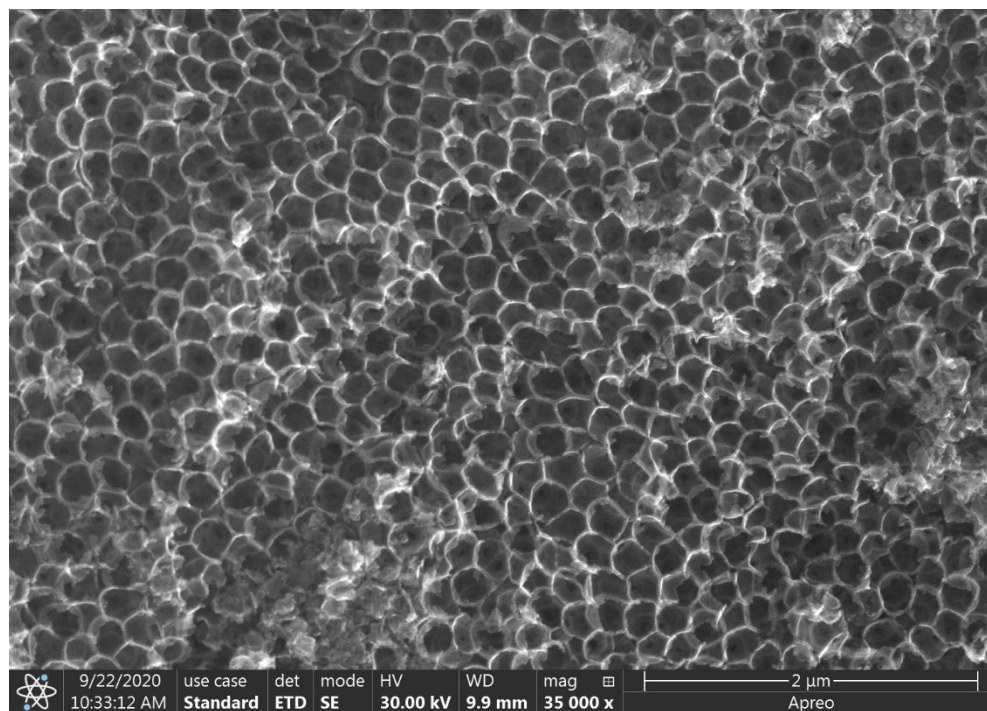


Fig. S7 Broken 3DOM porous structure of $\text{Cu}_3\text{N}(40)@3\text{DOM-TiO}_x\text{N}_y$.

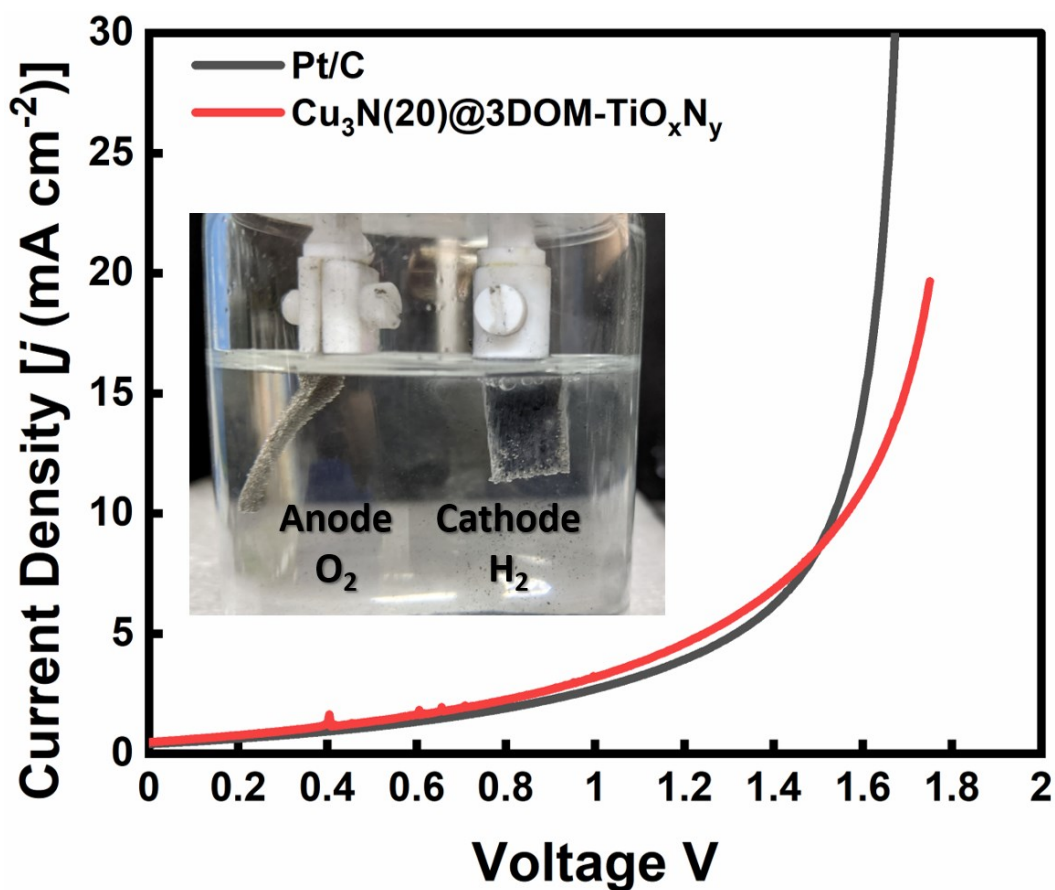


Fig. S8 Water splitting electrolyzer using $\text{Cu}_3\text{N}(20)\text{@}3\text{DOM-TiO}_x\text{N}_y$ electrocatalyst cathode.

The $\text{Cu}_3\text{N}(20)\text{@}3\text{DOM-TiO}_x\text{N}_y$ on nickel foam acted as the cathode and displayed a high performance with a cell voltage of 1.57 V, which is close to the 1.51 V of Pt/C to afford 10 mA cm^{-2} water splitting current in 1.0 M PBS with continuous gas evolution on both electrodes in a two-electrode water electrolyzer.

Additionally, a video showing the same two-electrodes electrolyzer driven by a 2V solar-panel generating H_2 bubbles can be found in the supporting material.

Table S1 Ti and Cu ratio obtained from ICP-OES test.

Element	Mass ratio wt (%)	Atomic Percentage (%)
Cu	13.74	20.8%
Ti	39.40	79.2%

Table S2 Surface area, pore distribution and pore volume comparison of $\text{Cu}_3\text{N}(20)@3\text{DOM-TiO}_x\text{N}_y$ and $\text{bulk-Cu}_3\text{N}(20)@TiO_xN_y$.

	$\text{Cu}_3\text{N}(20)@3\text{DOM-TiO}_x\text{N}_y$	$\text{Bulk-Cu}_3\text{N}(20)@TiO_xN_y$
Surface Area $\text{m}_2 \text{g}^{-1}$	163.7521	7.3568
Pore Volume $\text{cm}^3 \text{g}^{-1}$	0.260232	0.039090
Pore size nm	6.3567	21.25396

Table S3 Surface elemental weight ratio and atomic ratio of the C, N, O, Ti, Cu and Cl.

Element	Mass ratio wt/%
Cu	11.85
Ti	5.45
N	5.63
O	32.64
C	8.27
Cl	<0.1
Total	100.00

Table S4 HER performance comparison of several up to date related electrocatalysts.

Electrocatalyst	Electrolyte	Overpotential mV (@10mA cm ⁻²)	Tafel Slope mV dec ⁻¹	References
Pt/C	Universal pH	50~55	42~47	This work
Cu ₃ N@3DOM-TiO _x N _y	Universal pH	71.1~79.3	55~63	This work
Cu ₂ O-Cu ₂ Se nanoflake arrays	Universal pH	52.9~77.8	78.7~173.5	1
Cu-doped CoP arrays	Universal pH	81~137	102~144	2
Cu(0)-based catalyst	Neutral	70	127	3
MOF-derived copper nitride/phosphide	Neutral	109	69.0~138.3	4
Cu-Ti	Alkaline	108	~120	5
Mesoporous Cu-Ni	Alkaline	140	79	6
Holey Ni-Cu sheets	Alkaline	100	~70	7
NiMo-NiCu	Alkaline	154	42	8
Co ₃ O ₄ -CuO	Alkaline	288	65	9
Hierarchical nanoporous Ni(Cu)@NiFeP	Alkaline	128	121.8	10
Cu@Cu ₂ O@C	Alkaline	97	274~307	11
Cu-Mo-O nanosheets	Alkaline	112	136	12
Cu-MOF	Alkaline	89.3	33.4	13
Cu ₂ O layer/TiO ₂ nanodots	Alkaline	96	160	14
Cu-Co ₂ P/NCNTs	Acidic	140	112	15
Hollow Cu/Cu ₂ O/Cu ₂ S	Acidic	86	107	16
Cu ₃ P-CoP nanowire	Acidic	59	96	17
Cu-MoS ₂ /rGO	Acidic	126	90	18
Hemi-core@frame AuCu@IrNi	Acidic	355	58	19
Cu@graphdiyne core-shell nanowires array	Acidic	79	89	20
NiMo ₆ O ₂₄ @Cu/TNA	Acidic	130	89.2	21

References

1. Ray C, *et al.* Cu₂O–Cu₂Se mixed-phase nanoflake arrays: pH-universal hydrogen evolution reactions with ultralow overpotential. *ChemElectroChem* **6**, 5014-5021 (2019).
2. Wen L, *et al.* Cu-Doped CoP nanorod arrays: efficient and durable hydrogen evolution reaction electrocatalysts at all pH values. *ACS Applied Energy Materials* **1**, 3835-3842 (2018).
3. Liu X, Cui S, Sun Z, Du P. Robust and highly active copper-based electrocatalyst for hydrogen production at low overpotential in neutral water. *Chemical Communications* **51**, 12954-12957 (2015).
4. Wang Q, *et al.* MOF-derived copper nitride/phosphide heterostructure coated by multi-doped carbon as electrocatalyst for efficient water splitting and neutral-pH hydrogen evolution reaction. *ChemElectroChem* **7**, 289-298 (2020).
5. Shinde DV, *et al.* In situ dynamic nanostructuring of the Cu–Ti catalyst-support system promotes hydrogen evolution under alkaline conditions. *ACS Applied Materials & Interfaces* **10**, 29583-29592 (2018).
6. Li Z, *et al.* Mesoporous hollow Cu–Ni alloy nanocage from core–shell Cu@Ni nanocube for efficient hydrogen evolution reaction. *ACS Catalysis* **9**, 5084-5095 (2019).
7. Chu S, *et al.* Holey Ni-Cu phosphide nanosheets as a highly efficient and stable electrocatalyst for hydrogen evolution. *Applied Catalysis B: Environmental* **243**, 537-545 (2019).
8. Santos HLS, Corradini PG, Medina M, Dias JA, Mascaro LH. NiMo–NiCu inexpensive composite with high activity for hydrogen evolution reaction. *ACS Applied Materials & Interfaces* **12**, 17492-17501 (2020).
9. Tahira A, Ibupoto ZH, Willander M, Nur O. Advanced Co₃O₄–CuO nano-composite based electrocatalyst for efficient hydrogen evolution reaction in alkaline media. *International Journal of Hydrogen Energy* **44**, 26148-26157 (2019).
10. Sun Q, *et al.* Hierarchical nanoporous Ni(Cu) alloy anchored on amorphous NiFeP as efficient bifunctional electrocatalysts for hydrogen evolution and hydrazine oxidation. *Journal of Catalysis* **373**, 180-189 (2019).
11. Li N, Yan W, Zhang W, Wang Z, Chen J. Photoinduced formation of Cu@Cu₂O@C plasmonic nanostructures with efficient interfacial charge transfer for hydrogen evolution. *Journal of Materials Chemistry A* **7**, 19324-19331 (2019).
12. Wang A, *et al.* Dynamically controlled growth of Cu–Mo–O nanosheets for efficient electrocatalytic hydrogen evolution. *Journal of Materials Chemistry C* **8**, 9337-9344 (2020).
13. Nivetha R, *et al.* Cu based Metal Organic Framework (Cu-MOF) for electrocatalytic hydrogen evolution reaction. *Materials Research Express* **7**, 114001 (2020).
14. Long B, *et al.* Interface charges redistribution enhanced monolithic etched copper foam-based Cu₂O layer/TiO₂ nanodots heterojunction with high hydrogen evolution electrocatalytic activity. *Applied Catalysis B: Environmental* **243**, 365-372 (2019).
15. Pan Y, Liu Y, Lin Y, Liu C. Metal doping effect of the M–Co₂P/Nitrogen-doped carbon nanotubes (M = Fe, Ni, Cu) hydrogen evolution hybrid catalysts. *ACS Applied Materials & Interfaces* **8**, 13890-13901 (2016).

16. Wei Y, He W, Sun P, Yin J, Deng X, Xu X. Synthesis of hollow Cu/Cu₂O/Cu₂S nanotubes for enhanced electrocatalytic hydrogen evolution. *Applied Surface Science* **476**, 966-971 (2019).
17. Du H, Zhang X, Tan Q, Kong R, Qu F. A Cu₃P–CoP hybrid nanowire array: a superior electrocatalyst for acidic hydrogen evolution reactions. *Chemical Communications* **53**, 12012-12015 (2017).
18. Li F, *et al.* Synthesis of Cu–MoS₂/rGO hybrid as non-noble metal electrocatalysts for the hydrogen evolution reaction. *Journal of Power Sources* **292**, 15-22 (2015).
19. Park J, *et al.* Hemi-core@frame AuCu@IrNi nanocrystals as active and durable bifunctional catalysts for the water splitting reaction in acidic media. *Nanoscale Horizons* **4**, 727-734 (2019).
20. Xue Y, *et al.* Self-catalyzed growth of Cu@graphdiyne core–shell nanowires array for high efficient hydrogen evolution cathode. *Nano Energy* **30**, 858-866 (2016).
21. Zang D, Huang Y, Li Q, Tang Y, Wei Y. Cu dendrites induced by the Anderson-type polyoxometalate NiMo₆O₂₄ as a promising electrocatalyst for enhanced hydrogen evolution. *Applied Catalysis B: Environmental* **249**, 163-171 (2019).